Well-Dispersed Pt Catalysts Supported on Porous Carbon Nanofibers for Improved Methanol Oxidation in Direct Methanol Fuel Cells

Geon-Hyoung An and Hyo-Jin Ahn[z]

Department of Materials Science & Engineering, Seoul National University of Science and Technology, Seoul 139-743, Korea

Pt catalysts supported on porous carbon nanofibers (CNFs) were synthesized by a co-electrospinning followed by a reduction method, for improved methanol oxidation in direct methanol fuel cells (DMFCs). Pt catalysts supported on porous CNFs exhibit the highest electrocatalytic activity (524.09 mA/mg$_{Pt}$) and superior electrocatalytic stability as compared to Pt/conventional CNFs and commercial Pt/C (E-TEK), owing to the excellent dispersion of the Pt catalysts on the supporting porous CNFs. These results indicate that porous CNFs possessing a high specific surface area and a high total pore volume are promising candidates as supports for catalysts for improved methanol oxidation in DMFCs.
© 2014 The Electrochemical Society. [DOI: 10.1149/2.0061407ssl] All rights reserved.

Direct methanol fuel cells (DMFCs), comprising an anode, a cathode, an electrolyte, and a separating membrane, have received considerable interest for their use in various applications such as mobile homes, cabins, and boats owing to the attractive advantages they offer, including high energy density, low operation temperature, high methanol energy conversion efficiency, and low environmental toxicity.[1] In spite of these advantages, several problems, such as their relatively high costs, low utilization of the Pt catalysts, low electrocatalytic activity, CO poisoning of the catalysts, and methanol crossover, still remain.[2] Among all these problems, high and effective utilization of Pt electrocatalysts remains the main focus of research in order to improve anode performance. One of the many available strategies to solve these problems is to introduce a supporting material such as a carbon-based material (graphite, carbon nanotubes (CNTs), and carbon nanofibers (CNFs)), metal oxide-based material (TiO$_2$, SnO$_2$, Sn-doped In$_2$O$_3$ (ITO), and WO$_x$), or a conducting polymer (PEDOT, PDDA, and poly(N-acteylaniline)).[3] Among these supporting materials, carbon-based materials have recently attracted the interest of many researchers as supports for electrocatalysts owing to their unique structure and physical/chemical stability, in addition to their low costs and large surface areas.[4] Furthermore, CNFs particularly have been actively studied as promising supports because of their unique properties such as large surface areas (448 m^2/g), excellent electrical conductivity (10^5 S/cm), and excellent thermal and chemical stabilities.[5–7] Till now, much effort has been devoted on the synthesis and characterization of Pt catalysts supported CNFs for use in DMFCs.[8,9] However, a systematic approach for obtaining porous CNF supports in order to improve an electrocatalyst's activity toward methanol oxidation in DMFCs has been not studied hitherto. Hence, we synthesized Pt catalysts supported on porous CNFs with two different porosity levels using 4 wt% and 8 wt% of an Sn precursor, and have demonstrated the electrochemical performance of DMFCs comprising the Pt/porous CNF system we synthesized.

Experimental

Pt catalysts supported on porous CNFs were prepared by co-electrospinning followed by a reduction method. First, two different types of porous CNF supports were synthesized by a co-electrospinning technique discussed elsewhere.[5] All chemicals purchased from Sigma-Aldrich were used without further purification. For the core region to be processed by co-electrospinning, 4 wt% or 8 wt% tin(II) chloride dihydrate (SnCl$_2 \cdot$2H$_2$O, $\geq$ 99.995) and poly(vinylpyrrolidone) (PVP, M$_w$ = 1,300,000 g/mol) were dissolved in *N, N*-Dimethylformamide (DMF, 99.8%). For the case of shell region to be processed by co-electrospinning, polyacrylonitrile (PAN, M$_w$ = 150,000) and PVP were dissolved in DMF. Subsequently,

CNFs with embedded SnO$_2$ nanoparticles were synthesized using the carbonization at 800°C in a N$_2$. Subsequently, in order to obtain porous CNFs, SnO$_2$-embedded CNFs were subjected to a H$_2$-reduction method (N$_2$:H$_2$ = 9:1; v/v) at 600°C for 15 h. This treatment caused the Sn nanoparticles to agglomerate outside the porous CNFs. In order to simultaneously remove the agglomerated Sn particles from the CNF surface and form functional groups on the surface instead, an acid treatment using a mixture (1:1 (v/v)) of HF (52%) and HNO$_3$ (66%) was performed. To fabricate Pt catalysts supported on porous CNFs, a reduction method was employed. Porous CNFs were dispersed in a 1.12 mM H$_2$PtCl$_6 \cdot x$H$_2$O ($\geq$99.9%) solution in de-ionized (DI) water. Then, concentrated NaBH$_4$ solution (100 mg/mL), used as a reducing agent, was added into the above-mentioned solution. The resultant samples were washed several times using DI water, and then freeze-dried at −50°C to maintain metallic Pt phases. Also, for comparison, Pt electrocatalysts supported on conventional CNFs were prepared using electrospinning followed by a reduction method. Conventional CNFs were synthesized using only PAN and PVP without the addition of Sn precursors.[5] We prepared 40 wt% Pt catalysts supported on conventional CNFs, 40 wt% Pt catalysts supported on porous CNFs synthesized using 4 wt% Sn precursor, and 40 wt% Pt catalysts supported on porous CNFs synthesized using 8 wt% Sn precursor (referred to as Pt/CNF, sample A, and sample B henceforth).

The morphological and structural properties of the samples were examined by field emission-scanning electron microscopy (FESEM; Hitachi S-4800) and transmission electron microscopy (TEM; JEOL 2100F, KBSI Suncheon Center). The specific surface areas and pore volumes of the samples were performed using the Brunauer-Emmett-Teller (BET) measurements by N$_2$ adsorption at 77 K. The crystal structures of the samples were characterized by X-ray diffractometry (XRD, Rigaku D/MAX2500 V). Electrochemical performance tests were performed by means of a potentiostat/galvanostat (PGST302N by Eco Chemie, Netherlands), set up using a conventional three-electrode system comprising a glassy carbon electrode (0.07 cm^2, a working electrode), a Pt gauze (a counter electrode), and Ag/AgCl (saturated KCl, a reference electrode). The electrolyte used was a mixture of 0.5 M H$_2$SO$_4$ and 2 M CH$_3$OH aqueous solutions. The electrocatalytic oxidation of methanol was characterized by cyclic voltammetry (CV) at a scan rate of 50 mV/s in the range −0.2−1.0 V. The chronoamperometric curves were obtained in a 0.5 M H$_2$SO$_4$ + 2 M CH$_3$OH solutions at a constant voltage of 0.5 V for 2,000 s. For comparison, the commercial Pt/C (40 wt% Pt on Vulcan carbon, E-TEK) was prepared and tested using above-mentioned same procedures.

Results and Discussion

Figure 1 presents a schematic illustration of Pt catalysts supported on conventional CNFs (left) and Pt catalysts supported porous CNFs
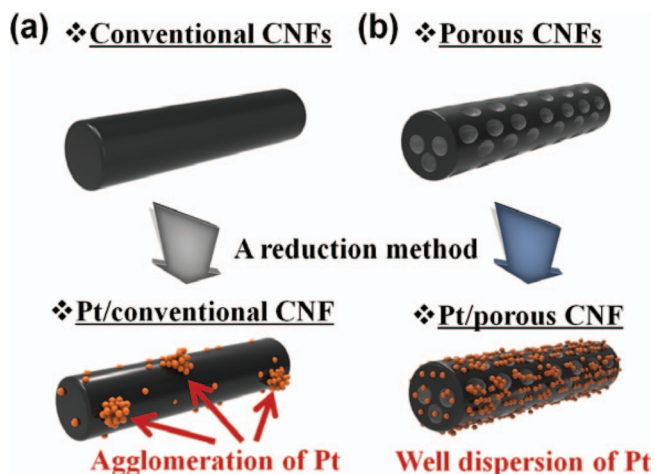
[z]E-mail: hjahn@seoultech.ac.kr

Figure 1. A schematic illustration of Pt catalysts supported on conventional CNFs (left) and Pt catalysts supported on porous CNFs (right) prepared using co-electrospinning followed by a reduction method.

(right). In the case of Pt/CNF, Figure 1a shows that the Pt catalysts are highly agglomerated on conventional CNFs, an observation in good agreement with previously reported literature.[10] This observation is in line with the well-known fact that it is difficult to get highly dispersed Pt catalysts on CNF supports. Our strategy for improving electrocatalytic oxidation of methanol by employing porous CNFs was to address and overcome exactly this problem; the result of employing our strategy, that is, the formation of the pores in CNFs, is shown in Figure 1b.

Figures 2a–2d show FESEM images of conventional CNFs, Pt/CNF, sample A, and sample B. The CNF diameters are observed to be 241−263 nm for conventional CNFs, 247−268 nm for Pt/CNF, 124−150 nm for sample A, and 119−138 nm for sample B. In the case of morphological properties of the samples, conventional CNFs and Pt/CNF exhibit smooth CNF surfaces, while samples A and B exhibit rough CNF surfaces, indicating the porous characteristics of the latter two samples. In addition, Pt/CNF and sample A shown in Figures 2b and 2c, respectively, indicate agglomerates of Pt electrocatalysts supported on CNFs because of strong carbon−carbon bonding. However, for sample B, no agglomerates of Pt catalysts were observed owing
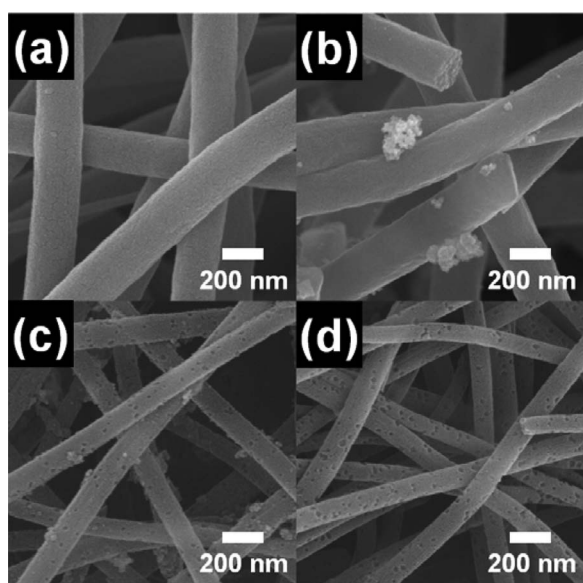

Figure 2. FESEM images of conventional CNFs, Pt/CNF, sample A, and sample B.
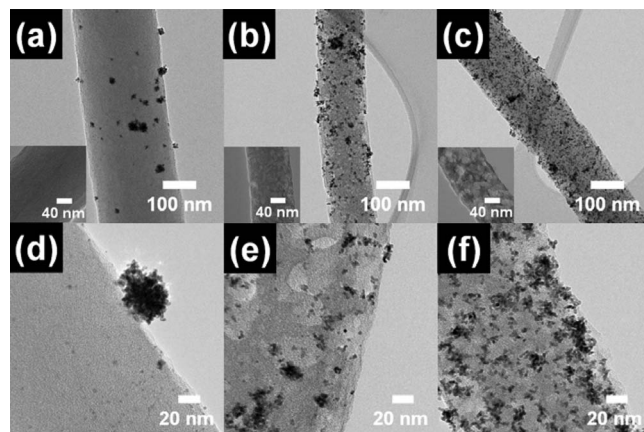

Figure 3. TEM images [(a)–(c)] and magnified TEM images [(d)–(f)] of Pt/CNF, sample A, and sample B.

to the excellent dispersion of Pt catalysts on the CNF supports. This is probably because of a higher loading of Pt catalysts caused by the higher porosity of sample B.

To further investigate the morphological properties of the samples, TEM measurements were carried out. Figure 3 shows TEM images [(a)–(c)] and magnified TEM images [(d)–(f)] of Pt/CNF, sample A, and sample B. As can be seen in Figure 3a, large agglomerates of Pt catalysts are sparsely distributed on conventional CNF supports. However, samples A and B exhibit excellent dispersion of Pt catalysts on porous CNF supports compared to the Pt/CNFs. In particular, total pore volumes and specific surface areas for conventional CNFs and porous CNF supports of samples A and B are 0.22 cm^3/g and 462 m^2/g, 0.48 cm^3/g and 865 m^2/g and 0.64 cm^3/g and 1082 m^2/g, respectively. This indicates that sample B exhibits greater porosity than sample A. Correspondingly, sample B exhibits an excellent dispersion of Pt catalysts, 2.6 nm−4.9 nm in size. This result indicates the possibility of improved electrocatalytic oxidation of methanol owing to the increase in the number of Pt catalysts active sites. This is in line with the well-known fact that excellent distribution of nanosized catalysts is a key factor for improving electrocatalytic activity and electrocatalytic stability of high-performance DMFCs. The TEM images of the porous CNF supports used in samples A and B, shown in the insets of Figures 3b and 3c, too prove that Porous CNF supports of sample B displays superior porous structures compared to porous CNF supports of sample A.

Figure 4 shows the XRD plots of conventional CNFs, Pt/CNF, sample A, and sample B. A broad diffraction peak is observed at 2θ
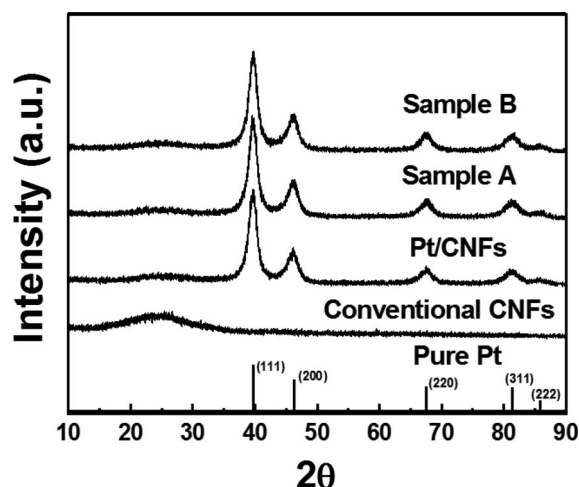

Figure 4. XRD plots of conventional CNFs, Pt/CNF, sample A, and sample B.
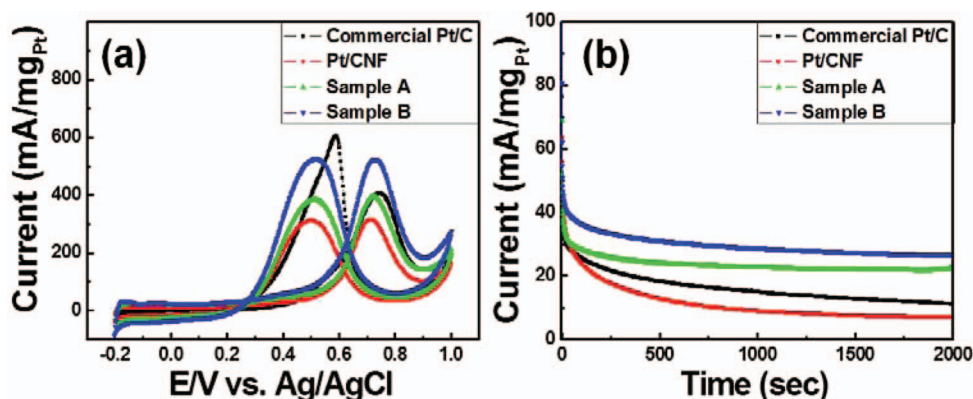
Figure 5. (a) Cyclic voltammograms (CV) of electrocatalytic oxidation of methanol using commercial Pt/C, Pt/CNF, sample A, and sample B catalysts. (b) Chronoamperometry (CA) of all samples characterized at 0.5 V in an aqueous solution of 0.5 M H_2SO_4 + 2 M CH_3OH for 2,000 s.

= ∼25°, indicating the (002) layer of graphite CNF. Characteristic diffraction peaks of Pt/CNF, sample A, and sample B are observed at 39.7°, 46.2°, 67.4°, and 81.3°, corresponding to the (111), (200), (220), and (311) planes of Pt, respectively, implying that the presence of metallic Pt phase with its face-centered cubic structure (space group *Fm3m*[225]) (JCPDS card No. 04–0802). In addition, in order to examine the grain sizes of the Pt catalysts, the diffraction peaks of sample B were calculated using the Scherrer equation given below:

$$D = 0.9\lambda/(\beta \cos \theta) \qquad [1]$$

where λ is the X-ray wavelength, β is the full width at half maximum (FWHM), and θ is the Bragg angle. The average sizes of Pt catalysts calculated using (111), (200), (220), and (311) planes are ∼4.8 nm for Pt/CNF, ∼4.6 nm for sample A, and ∼4.4 nm for sample B. These calculated values are in good agreement with the above-mentioned TEM results. Based on the FESEM, TEM, and XRD results, it can be inferred that Pt catalysts supported on porous CNFs were successfully synthesized.

Figure 5a shows cyclic voltammograms (CV) of electrocatalytic oxidation of methanol using commercial Pt/C, Pt/CNF, sample A, and sample B catalysts, performed at scan rate of 50 mV/s between −0.2 and 1.0 V (vs. Ag/AgCl) using an aqueous solution of 0.5 M H_2SO_4 + 2 M CH_3OH. In general, the electro-oxidation of methanol at the anode produces carbon dioxide, 6 protons, and 6 electrons (CH_3OH + H_2O → $6e^-$ + $6H^+$ + CO_2).[1] The oxidation efficiency of methanol is directly related to the anodic current density corresponding to forward peaks. In the case of forward peaks, the greater the number of electrons produced at the anode, higher the anodic current density, which, in turn, improves the efficiency of electro-oxidation of methanol in DMFCs. The anodic current density is calculated using the mass of Pt catalysts loaded on CNF supports. From an industry perspective, high mass activity of DMFCs is very important because of the cost of catalysts. Anodic current densities of commercial Pt/C, Pt/CNF, sample A, and sample B are 405.1 mA/mg$_{Pt}$, 315.0 mA/mg$_{Pt}$, 393.7 mA/mg$_{Pt}$, and 524.1 mA/mg$_{Pt}$, respectively. As can be seen, sample B shows the highest anodic current density among all samples, namely, approximately 1.29, 1.66 and 1.33 times higher than those of commercial Pt/C, Pt/CNF, and sample A, respectively. The highest anodic current density of sample B can be explained on the basis of the excellent distribution of Pt catalysts on porous CNF supports, which causes superior electrocatalytic activity owing to the increased electrolyte/catalyst contact area. These results indicate that porous CNFs (sample B) having a high surface area (1082 m²/g) can be used to obtain an excellent dispersion of Pt catalysts in order to improve much the electrocatalytic oxidation of methanol; this is a major advantage of using porous CNFs over commercial Pt/C and conventional CNF electrocatalysts.

To demonstrate the electrocatalytic stability of all samples during methanol oxidation, chronoamperometry (CA) measurements were performed at 0.5 V in an aqueous solution of 0.5 M H_2SO_4 + 2 M CH_3OH for 2,000 s, as shown in Figure 5b. When the potential was fixed at 0.5 V, the oxidation current decreased quickly during the initial stage owing to the accumulation of intermediate species such as CH_3OH_{ads} and CHO_{ads}. Such intermediate species were adsorbed on Pt catalysts, thus interrupting the oxidation reaction of methanol. Furthermore, a subsequent decrease in current decay was observed for all catalysts owing to the adsorption of SO_4^{2-} anions on the catalyst surface; this anion absorption hindered the electrocatalytic oxidation of methanol.[2] Despite the hindrance of anion absorption, among all samples, sample B maintained the highest current density during methanol oxidation owing to its excellent distribution of Pt catalysts supported on porous CNFs, which caused improved electrolyte/catalyst contact area. It is noted that well-dispersed Pt catalysts supported on porous CNFs exhibited the highest electrocatalytic oxidation effciency of methanol and excellent electrocatalytic stability in DMFCs compared to commercial Pt/C and Pt/CNF catalysts.

Conclusions

Pt catalysts supported on porous CNFs were successfully synthesized by co-electrospinning followed by a reduction method. The use of porous CNFs resulted in an excellent dispersion of Pt catalysts compared to conventional CNFs owing to increased specific surface areas and total pore volumes. Furthermore, an optimal amount of 8 wt% of Sn precursor was found to yield porous CNFs having the highest surface area (sample B, 1082.1 m²/g). Consequently, sample B exhibited the highest electrocatalytic activity (524.09 mA/mg$_{Pt}$) and superior electrocatalytic stability among all the samples tests: commercial Pt/C, Pt/conventional CNF, and Pt/porous CNF obtained using 4 wt% Sn precursor. The use of porous CNFs, which causes excellent dispersion of Pt catalysts, will hopefully be a promising tool for achieving high-performance DMFCs.

References

1. Y. S. Kim, S. H. Nam, H.-S. Shim, H.-J. Ahn, M. Anand, and W. B. Kim, *Electrochem. Commun.*, **10**, 1016 (2008).

2. G.-H. An and H.-J. Ahn, *J. Electroanal. Chem.*, **707**, 74 (2013).
3. S. Sharma and B. G. Pollet, *J. Power. Sourc.*, **208**, 96 (2012).
4. G.-H. An and H.-J. Ahn, *Ceram. Int.*, **38**, 3197 (2012).
5. G.-H. An and H.-J. Ahn, *Carbon*, **65**, 87 (2013).
6. T.-H. Park, J.-S. Yeo, M.-H. Seo, J. Miyawaki, I. Mochida, and S.-H. Yoon, *Electrochim. Acta*, **93**, 236 (2013).
7. G.-H. An and H.-J. Ahn, *Electrochem. Solid State Lett.*, **2**, M33 (2013).
8. M. Li, G. Han, and B. Yang, *Electrochem. Commun.*, **10**, 880 (2008).
9. S. Kang, S. Lim, D.-H. Peck, S.-K. Kim, D.-H. Jung, S.-H. Hong, H.-G. Jung, and Y. Shul, *Int. J. Hydrogen Energy*, **37**, 4685 (2012).
10. S. M. Andersen, M. Borghei, P. Lund, Y.-R. Elina, A. Pasanen, E. Kauppinen, V. Ruiz, P. Kauranen, and E. M. Skou, *Solid State Ionics*, **231**, 94 (2013).